CHAPTER IX.E

EFFECT OF VAPOR-LIQUID EQUILIBRIUM ON FISCHER-TROPSCH HYDROCARBON SELECTIVITY FROM A SLURRY REACTOR FOR A DEACTIVATING CATALYST

ABSTRACT

The results for the Fischer-Tropsch reaction carried out in the slurry phase over an iron-based catalyst which deactivates linearly following a period of constant activity are reported. Experimentally obtained hydrocarbon selectivity plots exhibit a single value of chain growth probability, a, at short times on stream while two values of chain growth probability are observed at longer times on stream (during catalyst deactivation). This is shown to be consistent with a vapor-liquid equilibrium (VLE) phenomena in the slurry reactor. An unsteady-state VLE model is developed which successfully predicts the two values of chain growth probability (positive deviations) at longer times on stream even though single-a stoichiometry is assumed. This is shown to be due to the "flashing off" of previously accumulated lighter hydrocarbons along with the hydrocarbons produced at the longer times on stream. The model also predicts the increase in the extent of the positive deviations or the value of the second chain growth probability with increasing times on stream The model adequately predicts the hydrocarbon selectivity at short times on stream and the values of the second chain growth probability at longer times on stream. However, the model over predicts the number of carbon atoms at which the break in the selectivity plots is observed probably due to inadequate estimates of hydrocarbon saturation vapor pressures and the assumption of the ideal gas law.

INTRODUCTION

The Fischer-Tropsch (FT) synthesis consists of the reaction of carbon monoxide with hydrogen to produce hydrocarbons with a wide range of molecular weights. The FT reaction is generally regarded as being similar to a polymerization reaction wherein C_1 monomer units are added stepwise to a growing hydrocarbon chain on the catalyst surface. Based on this reasoning, the hydrocarbon selectivity of the FT reaction is given by the well-known Anderson-Schulz-Flory (ASF) reaction mechanism which relates the mole fraction, m, of a hydrocarbon possessing i carbon atoms as

$$m_i = \alpha m_{i-1} = (1-\alpha)\,\alpha^{i-1} \qquad (1)$$

The hydrocarbon selectivity is, thus, dependent upon a single parameter, a, which is termed as the probability of chain growth and is independent of the number of carbon atoms in the growing hydrocarbon chain. If the logarithm of mole fraction of hydrocarbons is plotted against the number of carbon atoms, then according to Equation (1), the result should be a single straight line with a slope given by a.

However, results from a number of research groups (for example, IX.E-1 - IX.E-3) show that experimentally obtained hydrocarbon selectivities deviate from that predicted by the ASF mechanism. A schematic of the experimentally obtained selectivity plots is shown in Figure IX.E-1. Three regions in Figure IX.E-1 can be identified: up to hydrocarbons possessing about 8 to 12 carbon atoms the selectivity plot yields a straight line with a slope given by one value of a, a_1; between hydrocarbons possessing 12 to 25 carbon atoms the selectivity plot yields another straight line with a different and greater slope, a_2 (so-called positive deviations from the ASF mechanism); for hydrocarbons possessing greater than 25 carbon atoms the

experimental data exhibit a lower mole fraction than expected (so-called negative deviations from the ASF reaction mechanism). Further, the extent of negative deviations have been observed to decrease with reactor time on stream while the extent of positive deviations has been observed to increase with time on stream (IX.E-4).

The negative deviations from the ASF reaction mechanism have been previously ascribed to vapor-liquid equilibrium (VLE) phenomena in a slurry phase FT reactor (IX.E-4, IX.E-5). It has been shown that the higher molecular weight hydrocarbons formed during the FT reaction are preferentially retained in the reactor slurry and do not leave the reactor with the lighter hydrocarbons in the exit vapor stream (IX.E-4, IX.E-5). This causes a negative deviation in the observed selectivity plot which consists only of the hydrocarbons in the exit vapor stream of the FT reactor.

On the other hand, the positive deviation from the ASF reaction mechanism, i.e. the second a of the selectivity plots, has not been ascribed to VLE phenomena. Other explanations offered for the positive deviations or the second a value include: (i) two-site catalyst model (IX.E-1, IX.E-3), (ii) diffusion-enhanced olefin readsorption model (IX.E-7), and (iii) olefin-readsorption with increased hold-up model (IX.E-8).

In this study, we show how VLE phenomena in a slurry phase FT reactor can account for the positive deviations from the ASF reaction mechanism (double-a selectivity) for the special case of a catalyst which possesses constant activity for a while after which it deactivates. Such a case is quite common in laboratory testing of FT catalysts (see for example refs. (IX.E-9, IX.E-10)) wherein constant catalyst activity

is achieved only for a limited time. Experimental hydrocarbon selectivity plots are obtained in this study using an iron based catalyst in a slurry phase FT reactor operated for a time on stream (TOS) of 30 days. An unsteady-state VLE model is developed for a slurry phase reactor which predicts the observed positive deviations (double-a) in the hydrocarbon selectivity. We also show that VLE phenomena can explain the increase in positive deviations with increasing reactor TOS as the extent of catalyst deactivation increases.

EXPERIMENTAL

Reaction System

The FT reaction is carried out in a 1 liter stirred autoclave reactor. CO and H_2 are metered separately and pre-mixed in a 0.5 liter vessel before being fed to the reactor. The vapor phase products exit the reactor at the top, then through a fritted filter and pass through two traps in series. The first trap is maintained at 100°C while the second is maintained at 0°C. The uncondensed gases from these two traps pass through a back pressure regulator to a soap bubble flow meter that is utilized for measuring the flow of the exit gas. The uncondensed gases are periodically sampled and analyzed by on-line gas chromatographs.

Product Analysis

The composition of the uncondensed product gases are obtained using two on-line gas chromatographs. The first is a Carle Gas Analyzer (Hach Series 400 A) which is used to obtain the mole fractions of CO, H_2, CO_2 and C_1 to C_4 hydrocarbons. The second on-line gas chromatograph is a Hewlett Packard 5790A with a Porapak Q column using a thermal conductivity detector, is used to obtain the mole fractions of C_4 to about C_9 hydrocarbons in the uncondensed product gases.

The condensed liquid products are separated into an aqueous and a hydrocarbon phase. The aqueous phase is analyzed in the Hewlett Packard 5790A described above. The hydrocarbon phase is analyzed using a Hewlett Packard 5890 Series II gas chromatograph with a DB-5 capillary column and a flame ionization detector.

Procedure

The iron-based catalyst used was obtained from United Catalysts, Inc. (UCI #1185-78) that was prepared as part of a catalyst selection program for Run 2 at the LaPorte, Texas pilot plant. The catalyst (36.4 g) is loaded into the reactor with 300 g of C_{28} paraffin as the start-up solvent. Pretreatment of the catalyst is carried out using CO at 270°C and a pressure of 12.9 atm for 24 hours. Subsequently, the flow of synthesis gas is started at a flow rate of 2.5 moles/hr with a H_2/CO molar ratio of 0.7. The reaction conditions are the same as for pretreatment: 270°C and 12.9 atm. These conditions are maintained throughout the run lasting for 720 hours.

EXPERIMENTAL RESULTS

Figure IX.E-2 shows the conversions of synthesis gas (CO + H_2) as a function of TOS of the reactor. The conversions remains fairly constant for a period of about 250 hr after which the catalyst deactivates and the conversion decreases. The decrease in conversion is approximately linear as shown in Figure IX.E-2.

Figure IX.E-3 shows the hydrocarbon selectivities at different reactor TOS. The plots at shorter TOS (48 and 240 hours) exhibit only a single straight line with slope a of 0.65. (Note that negative deviations from the ASF plot do occur but this is due to the hold up of the heavier hydrocarbons as shown in previous studies (IX.E-4, IX.E-

5)). Positive deviations from the ASF mechanism are not exhibited. Hence, the hydrocarbon selectivity appears to follow the ASF reaction mechanism at short reactor TOS.

In contrast, however, the plots at longer TOS (456 and 552 hours) exhibit positive deviations from the ASF mechanism. The selectivity is characterized by two straight lines with different slopes, a_1 and a_2. The value of a_1 for the selectivity at longer TOS is the same as the single value of a at short TOS, i.e., 0.65. The value of a_2 is greater than the value of a_1 (0.74 to 0.81). The selectivity plots at longer TOS are similar to those reported by other investigators over iron-based catalysts with about the same values of a_1 and a_2 (IX.E-1 - IX.E-3).

Further, Figure IX.E-3 shows that the extent of the positive deviations (or the value of the slope a_2 at longer TOS) increases with reactor TOS. Thus the value of a_2 at a TOS of 456 hours is 0.74 while at a TOS of 552 hours the value of a_2 is greater (0.81). The break in slope between a_1 and a_2 or the number of carbon atoms at which the onset of the positive deviations occur is approximately 12 to 14. This is also similar to double-a plots obtained by other investigators for iron-based catalysts.

It is significant that the onset of positive deviations corresponds to the TOS at which the catalyst starts deactivating. For the period of constant conversion (TOS less than 250 hrs), the selectivity plots correspond to those expected according to the ASF reaction mechanism (single-a).

The change in the nature of hydrocarbon selectivity exhibited (single-a to double-a) by the catalyst with reactor TOS cannot be readily explained by existing theories of positive deviations from the ASF mechanism. In the following sections we

develop a VLE model of a slurry phase FT reactor to investigate whether it can explain the experimental results.

VLE MODEL DEVELOPMENT

Unsteady state nature of reactor

A stirred tank slurry reactor wherein the catalyst is suspended in an inert solvent (usually a heavy paraffin) is commonly used in FT experimental studies. Usually only the vapor phase products (under reaction conditions) are collected overhead from the reactor for analysis; reactor liquid phase material may be withdrawn at intervals if this operation is necessary. These vapor phase products leaving the reactor are merely those which are in thermodynamic equilibrium with the liquid phase remaining in the reactor.

It has been recognized that laboratory reactors operate in an unsteady state mode with respect to liquid phase and gas phase compositions (IX.E-4, IX.E-11) even in the case of a catalyst with constant activity. For example, in a study (IX.E-4) conducted with C_{28} paraffin as the start-up solvent, the composition of the reactor liquid determined after several hundred hours of reactor TOS was found to be only 50 wt.% C_{28} with the rest consisting of hydrocarbon products from the FT reaction. Hence, during the reaction the composition of the liquid phase in the reactor changes with TOS and thus the composition of the vapor phase which is in thermodynamic equilibrium with the liquid phase also changes with TOS.

In addition to the change in liquid and vapor phase compositions, the amount of liquid in the reactor can increase or decrease with TOS depending upon the reaction conditions of temperature and pressure as well as the composition of the

start-up oil. Hence, a model of the composition of the exit vapor phase products from a slurry reactor must take into consideration the inherent unsteady state nature of the reactor.

A schematic illustrating the development of the model is shown in Figure IX.E-4. Two separate parts of the model can be distinguished: reaction stoichiometry and VLE. In the first part a specific stoichiometry of the FT reaction is assumed to obtain the total molar flow rate as well as the mole fractions of each individual hydrocarbon produced by the reaction. The products that are formed are assumed to intimately mix with the liquid phase already present in the reactor with the establishment of thermodynamic vapor-liquid equilibrium. The composition of the exit vapor phase product hydrocarbons are calculated in the second part of the model assuming thermodynamic equilibrium between the vapor phase products and liquid remaining in the reactor.

Reaction stoichiometry

The reaction stoichiometry followed in this model closely parallels that developed in a previous study (IX.E-11). Two major assumptions are made:

1. The ASF distribution, i.e., hydrocarbon selectivity described by a single value of a is assumed. Hence the mole fractions of individual hydrocarbons relative to the total amount of hydrocarbons formed, m_i, are given by Equation (1).

2. The hydrocarbon products consist exclusively of paraffins. This assumption is a matter of convenience as the parameters needed for the VLE have been well documented for paraffins. Moreover, the hydrocarbon products, especially C_{20+}, consist mainly of paraffins for iron-based catalysts (IX.E-12).

The FT reaction can then be written as

$$(2n+1)H_2 + nCO \rightarrow C_nH_{2n+2} + nH_2O \quad (2)$$

where n is the average number of carbon atoms in the hydrocarbon products. It has been reported (for example, IX.E-11) that the average number of carbon atoms in the hydrocarbon product is related to the value of a,

$$n = 1/(1 - \alpha) \quad (3)$$

Further, the water gas shift reaction plays an appreciable role for iron-based catalysts,

$$CO + H_2O \rightarrow CO_2 + H_2 \quad (4)$$

If F' is the total molar flow rate of hydrogen and carbon monoxide to the reactor and n_{HC} the molar rate of CO forming hydrocarbons then the molar flow rate of products and unconverted reactants after reaction, F, is given as

$$F = F' - 2n_{HC} \quad (5)$$

Equation (5) indicates that there is a decrease in the total number of moles during the FT reaction. The decrease in moles is expected to be greater with increasing conversion and early results for Fischer-Tropsch conversions were frequently reported on the basis of gas contraction (IX.E-13).

If X_{CO+H_2} is the conversion of synthesis gas in the reactor, then (IX.E-11)

$$n_{HC} = F'X_{CO+H_2}/(4-\alpha) \quad (6)$$

and z_{HC}, the total mole fraction of hydrocarbons in the product is (IX.E-11)

$$z_{HC} = n_{HC}(1-\alpha)/F \quad (7)$$

Since the hydrocarbon products are assumed to follow an ASF distribution (Equation (1)), the mole fractions of individual hydrocarbons possessing i number of carbon atoms is given as

$$z_i = (1-\alpha)\,\alpha^{i-1} z_{HC} \tag{8}$$

Hence, the total molar flow rate of products (and unconverted reactants), F, and the mole fractions of individual hydrocarbons can be calculated from the input molar flow rate of synthesis gas, F', and the synthesis gas conversion, X_{CO+H_2}.

Vapor-liquid equilibrium

In the second part of the model, the products from the reaction are assumed to intimately mix with the liquid phase already present in the reactor establishing thermodynamic vapor-liquid equilibrium. The vapor-phase products exiting the reactor are then in equilibrium with the liquid phase remaining in the reactor. The assumptions made are:

1. CO, H_2, H_2O and CO_2 are assumed to be negligibly soluble in the liquid phase in the reactor. Hence their mole fractions in the liquid phase are zero.

2. No liquid is withdrawn from the reactor, i.e., only vapor phase products exit the reactor.

3. The reactor is in the unsteady state mode, i.e., the number of moles in the reactor liquid, Q, the molar flow rate of vapor phase products, V, and the mole fractions of components in the vapor, y_i, and in the liquid phase, x_i, change with reactor TOS.

4. The vapor is assumed to follow the ideal gas law and the liquid is considered to behave as an ideal mixture. Hence the mole fractions in the vapor and liquid phase are related by

$$P\, y_i = x_i P^s i \tag{9}$$

For an infinitesimally small interval of time Δt, a material balance for all components (including CO, H_2, CO_2, H_2O) gives

$$\Delta Q = Q - Q_{prev} = F\Delta t - V\Delta t \tag{10}$$

A material balance for a hydrocarbon component possessing i carbon atoms can be written as

$$z_i F\Delta t + Q_{prev} x_{prev,i} = V\, y_i \Delta t + Q x_i \tag{11}$$

Simplifying Equations (9), (10) and (11), we get,

$$x_i = (z_i F\Delta t + Q_{prev} x_{prev,i})/((F - Q + Q_{prev})\ (P^s i/P)\ \Delta t + Q) \tag{12}$$

Another relationship is obtained by recognizing that the sum of all hydrocarbon mole fractions in the liquid phase is zero.

$$\Sigma x_i = 1 \tag{13}$$

Equations (9), (12) and (13) completely describe the VLE part of the model. From a knowledge of the initial conditions (at t=0) the mole fractions of the hydrocarbons in the liquid phase, x_i, and in the vapor phase, y_i, can be calculated at any TOS.

MODEL SIMULATION

The unsteady state VLE model developed in an earlier section is utilized with experimentally known initial values of parameters and conversions to investigate whether the above experimental hydrocarbon selectivity can be predicted.

Initial values of the mole fractions of hydrocarbons in the liquid are zero except for C_{28} (start-up oil) which has a mole fraction of one. The initial number of moles in the liquid is 0.711 corresponding to 300 g of C_{28}. The total feed synthesis gas flow rate, F', is 2.5 moles/hr as maintained experimentally. Based upon the results shown in Figure IX.E-2, the conversion of synthesis gas is assumed to be constant for the first 250 hrs at 88%. After the first 250 hrs, the synthesis gas conversion is assumed to vary linearly from 88% to 35% at the end of 720 hrs. The number of hydrocarbon components of differing numbers of carbon atoms is chosen to fall in the range C_1 to C_{100}. For the values of α required to represent the data the sum of the mole fractions of C_{100+} products is negligible compared to the fraction falling in the C_1 to C_{100} range. The value of the small time interval Dt used for Equation (12) is 0.01 hours.

The VLE model requires the saturation vapor pressures of each hydrocarbon component from a hydrocarbon containing one carbon atom (methane) to a hydrocarbon containing 100 carbon atoms. Accurate experimental saturation vapor pressures at the reaction conditions used in this study are, however, not available, especially for the heavier hydrocarbons. Hence estimates of the saturation vapor pressures are used in the model simulation. These are taken from two sources:

1. A correlation from a previous study (IX.E-11) where the saturation vapor pressure of each hydrocarbon component (paraffin) possessing i carbon atoms is given as

$$P^s i = P_0 \beta^{i-1} \tag{14}$$

where

$$P_0 = 1.78382 \; x \; 10^4 kPa \tag{15}$$

$$\beta = \exp(-427.218(1/T - 1.029807 \; x \; 10^{-3})) \tag{16}$$

This correlation has been shown to hold valid for paraffins possessing 5 to 30 carbon atoms (IX.E-11). For the purposes of this study the correlation is assumed to hold true for heavier hydrocarbons as well.

2. From coefficients of the Antoine's vapor pressure equation given for paraffins (IX.E-14) by the API Project 44. These coefficients have been given for hydrocarbons at low total pressures (0.1 to 2 atm) which is much lower than the reaction pressure used in this study (12.9 atm). For the purposes of this study we assume that same coefficients can be used at the higher reaction pressure of 12.9 atm.

A comparison of these two sources of saturation vapor pressures at the reaction temperature of 270°C is shown in Figure IX.E-5. The two sources of saturation vapor pressure data agree well for hydrocarbons possessing 5 to 40 carbon atoms. Outside this range, however, the saturation vapor pressures calculated from these two sources deviate from each other.

Model predictions

Figure IX.E-6 shows the calculated molar flow rate of the exit vapor phase, V, as a function of reactor TOS. The vapor flow rate is constant up to a TOS of 250 hrs after which it linearly increases. This is related to the fact that the catalyst deactivates after 250 hrs and the synthesis gas conversion decreases. Since there is a net

decrease in the total number of moles during the FT reaction (Equation (5)), a decrease in conversion is expected to increase the molar flow rate after reaction. Further, an examination of Equations (5) and (6) shows that the expected increase in molar flow rate is linear. Both sources of saturation vapor pressures give similar values of the vapor flow rate. This is to be expected since the two sources differ mainly for C_{40+} hydrocarbons which are produced only in small quantities and, as shown below, remain mainly in the reactor.

Figure IX.E-7 shows the calculated moles of the liquid remaining in the reactor as a function of TOS. The moles of liquid in the reactor increases slightly at the beginning of the run and then continuously decreases. Hence, there is a net outflow of the liquid from the reactor with TOS under the conditions of this study. The rate of decrease in the amount of liquid is greater after the catalyst starts deactivating. This is understandable since a decrease in conversion leads to an increase in the total number of moles after reaction which would tend to carry away a greater amount of liquid from the reactor. The two saturation vapor pressure sources give different values of the moles in the liquid phased though the nature of the two curves are similar.

Figure IX.E-8 shows the calculated weight fraction of C_{28} in the reactor liquid with TOS. The C_{28} weight fraction decreases sharply at the beginning of the run followed by a period of slower decrease. Once the catalyst starts deactivating (TOS > 250 hrs), the weight fraction of C_{28} increases again. This will be referred to later. Again the nature of the curves are similar for the two sources of saturation vapor pressure sources used though the actual values differ.

The vapor phase hydrocarbon compositions, as predicted by the VLE model, are shown in Figures IX.E-9 and IX.E-10 at various TOS. Figure IX.E-9 corresponds to the vapor phase compositions calculated using the API Project 44 (IX.E-14) saturation vapor pressures while Figure IX.E-10 corresponds to the vapor phase compositions calculated using Equation (14). Several features of these plots are of interest.

The VLE model predicts the presence of negative deviations from the ASF mechanism at high numbers of carbon atoms at all TOS. This is similar to the results of previous VLE models (IX.E-4, IX.E-5). The VLE model predicts the absence of positive deviations at short TOS (48 and 240 hours) before the catalyst starts deactivating as observed experimentally. This is not surprising as the ASF mechanism (single-a) is assumed for the reaction stoichiometry in the VLE model.

More importantly, the VLE model predicts the presence of positive deviations from the ASF mechanism at longer times on stream (456 and 552 hours), after the catalyst starts deactivating, as observed experimentally. These positive deviations result in selectivity plots with two values of a as shown in Figure IX.E-9. Note that the VLE model assumes the ASF mechanism (single a) for the reaction stoichiometry. Hence, the presence of two values of a can be attributed to VLE phenomena. Further, the extent of positive deviations or the values of a_2 are predicted by the VLE model to increase with reactor TOS similar to experimental observations. Thus the value of a at a TOS of 456 hours is 0.72 while that at 552 hours is 0.78 in Figure IX.E-9. These values are quite similar to those observed experimentally at the same TOS (Figure

IX.E-3). Thus, the VLE model is able to predict all the features of the experimentally observed hydrocarbon selectivity plots and their variation with TOS of the reactor.

The reason for the positive deviations from the ASF mechanism can best be discerned from a combination of Figure IX.E-8 and Figure IX.E-11, which is a plot of the liquid phase compositions with reactor TOS (considering API 44 saturation vapor pressures). At short TOS there is a rapid accumulation of hydrocarbon products in the reactor liquid which results in the lowering of the mole fraction of the start-up oil (C_{28}) as shown in Figure IX.E-8. Even though the reactor liquid consists of 95 mole% C_{28}, a significant amount of hydrocarbon products are retained in the reactor liquid (Figure IX.E-11). As the reactor TOS increases there is a gradual build-up of these hydrocarbon products in the reactor as evidenced by the further decrease in the mole fraction of C_{28} (Figure IX.E-8). After the catalyst starts deactivating, the molar flow rate after reaction increases (Figure IX.E-6) causing the preferential "flashing off" or "stripping" of the comparatively lighter hydrocarbons from the reactor liquid. This is shown by the increase in the weight fraction of C_{28} with time on stream (Figure IX.E-8) and by the decrease in the mole fractions of lighter hydrocarbons in the reactor liquid (Figure IX.E-11). These hydrocarbons which "flash off" leave the reactor in the vapor phase along with the vapor phase products from the reaction produced during this time period and cause a positive deviation in the selectivity plot in the range of intermediate molecular weight hydrocarbons.

As the catalyst deactivates even further, the molar flow rate after reaction keeps increasing, causing more and more of the previously accumulated hydrocarbon products to "flash off," causing an increase in the extent of positive deviations. This is

shown by the increasing weight fractions of C_{28} (Figure IX.E-8) in the reactor liquid as well as the decreasing mole fractions of lighter hydrocarbons in the reactor liquid (Figure IX.E-11) with TOS.

The vapor phase compositions calculated using the two different sources of saturation vapor pressure are seen to be quite similar from a comparison of Figures IX.E-9 and IX.E-10. Both sources exhibit positive deviations (double-a selectivities) and their increase with TOS. However, the extent of positive deviations and the slopes of a_2 are greater when saturation vapor pressures from API Project 44 (IX.E-14) are used.

Comparison of experimental and theoretically predicted selectivity plots

A quantitative comparison of the experimental data with the model predictions is shown at short TOS in Figure IX.E-12 and at various longer TOS in Figures IX.E-13 to IX.E-16. Only the vapor phase compositions calculated from saturation vapor pressures from API Project 44 (IX.E-14) are shown for the sake of clarity. Figure IX.E-12 shows that the VLE model adequately predicts the experimental data quantitatively at short TOS. There is, however, a small discrepancy in the carbon number at which the onset of negative deviations are predicted and experimentally observed.

At longer TOS (during catalyst deactivation), there is a striking qualitative similarity between the experimental data and the VLE model predictions (Figures IX.E-13 to IX.E-16) in the extent of positive deviations from the ASF mechanism and in the shape of the selectivity curves. Further, the values of the second chain growth probability, a_2, predicted by the VLE model at various long TOS are quite close to

those experimentally observed values as shown in Table IX.E-1. There is, however, a significant over prediction of the break in the selectivity plot by the VLE model. Figures IX.E-13 to IX.E-16 show that the break in the selectivity plot is predicted to occur at a heavier hydrocarbon (C_{19}) than experimentally observed (C_{14}).

Table IX.E-1

Values of Second Slope α_2 from Experimental Data and Predicted by the VLE Model at Various Times on Stream

Time on Stream (Hrs)	Value of α_2 from Experimental Data	Value of α_2 Predicted by VLE Model
312	0.689	0.674
456	0.740	0.721
504	0.789	0.763
552	0.814	0.780

One possible reason for the over prediction of the break point is that the temperature at which VLE is established is different from the reaction temperature. In an earlier VLE study (IX.E-4), a much lower temperature had to be assumed for VLE in order to quantitatively predict the negative (not positive) deviations from the ASF mechanism. Figure IX.E-17 shows the calculated vapor phase compositions at a reactor TOS of 552 hours assuming different temperatures for VLE. This figure shows that the location of the break point depends on the temperature of VLE assumed. For example, the break point occurs at a hydrocarbon possessing 17 carbon atoms for a VLE temperature of 240°C and it occurs at an even lighter hydrocarbon (C_{14}) for a VLE temperature of 200°C. However, as the VLE temperature decreases the extent of the positive deviations decrease to a significant extent. Hence, this is probably not the only reason for the over prediction of the break point.

A second reason for the over prediction of the break point is the extrapolation necessary in order to estimate the saturation vapor pressures of hydrocarbons at reaction conditions. As noted earlier, experimental data for hydrocarbon vapor pressures at reaction conditions are not available.

A third reason for the over prediction of the break point is the assumption of the ideal gas law. This is a major assumption considering the range of hydrocarbons for which it is considered to be valid. For example, hydrocarbons possessing less than 8 carbon atoms have critical temperatures greater than the reaction temperature, i.e. these hydrocarbons are in the supercritical state. Conversely, for hydrocarbons possessing greater than 20 carbon atoms the critical pressure is less than the reaction pressure. The deviations from the ideal gas law in both these regions are expected to be quite large.

In summary, the VLE model predicts all the features of the experimentally obtained hydrocarbon selectivities, and especially the positive deviations from the ASF mechanism or the double-a selectivities. The VLE model also quantitatively predicts the value of the second chain growth probability, a_2, and its increase with reactor TOS. The location of the break point in the selectivity plot is over predicted by the VLE model probably due to inadequate estimates of saturation vapor pressures and/or the assumption of the ideal gas law.

CONCLUSIONS

Experimental hydrocarbon selectivities are obtained from a slurry FT reactor over an iron-based catalyst which maintains a constant activity for 250 hours after which it continuously deactivates. The selectivity plots at short TOS (during the period of constant activity) follow the well known ASF mechanism and are characterized by a

single chain growth probability . However, positive deviations from the ASF mechanism or double-a selectivity plots are observed at longer TOS (during the period of continuous deactivation). These double-a selectivity plots are similar to selectivity plots obtained by other investigators over iron-based catalysts.

An unsteady-state vapor-liquid equilibrium model is developed for the slurry FT reactor which takes into account the variation of amount of reactor liquid and hydrocarbon compositions of the vapor and liquid phases in the reactor. The VLE model is able to predict all the features of the experimental hydrocarbon selectivity plots. In particular, the model predicts the positive deviations or the double-a character of the selectivity plots and the increase in the extent of the positive deviations (value of a_2) with TOS during catalyst deactivation. The positive deviations are predicted to occur even though single-a, i.e., the ASF mechanism, is assumed for the reaction stoichiometry.

The reason for the occurrence of positive deviations is the VLE phenomena associated with the slurry reactor. At short TOS significant quantities of lighter hydrocarbons (as well as heavier hydrocarbons) accumulate in the liquid phase in the reactor. During catalyst deactivation, the molar flow rate after reaction increases causing a preferential "flashing off" of the previously accumulated lighter hydrocarbons. Thus the exit vapor stream consists not only of the hydrocarbons produced during that time but also the extra lighter hydrocarbons which are stripped from the reactor liquid causing the positive deviations from the ASF mechanism.

The calculated vapor phase compositions are strikingly similar to those experimentally observed at various TOS. The extent of positive deviations and the values of the second a are predicted quite well by the VLE model. However, the VLE

model over predicts the break point in the double-a plots at long TOS. Possible reasons for the overprediction include the unavailability of experimental hydrocarbon saturation vapor pressures at reaction conditions and the assumption of the ideal gas law.

The prediction of double-a selectivity plots by the VLE model, even though the single-a ASF stoichiometry is assumed, indicates that vapor-liquid equilibrium phenomena are responsible for the occurrence of the double-a hydrocarbon selectivity in the case of a deactivating catalyst.

ACKNOWLEDGMENT

This work was supported by U.S. DOE contract number DE-AC22-91PC90056 and the Commonwealth of Kentucky.

REFERENCES

IX.E-1. G.A. Huff and C.N. Satterfield, *J. Catal.*, **85**, 370 (1984).

IX.E-2. D.B. Bukur, D. Mukesh and S.A. Patel, *Ind. Eng. Chem. Res.*, **29**, 194 (1990).

IX.E-3. K. Herzog and J. Gaube, *J. Catal.*, **115**, 337 (1989).

IX.E-4. G.A. Huff, Ph.D. Dissertation, Massachusetts Institute of Technology, (1982).

IX.E-5. R.A. Dictor and A.T. Bell, *Ind. Eng. Chem. Proc. Des. Dev.*, **22**, 678 (1983).

IX.E-6. T.J. Donnelly, I.C. Yates and C.N. Satterfield, *Energy & Fuels*, **2**, 734 (1988).

IX.E-7. E. Iglesia, S.C. Reyes and R.J. Madon, *J. Catal.*, **129**, 238 (1991).

IX.E-8. W. Zimmerman, D.B. Bukur and S. Ledakowicz, *Chem. Eng. Sci.*, **47**, 2707 (1992).

IX.E-9. T.J. Donnelly and C.N. Satterfield, *Appl. Catal.*, **52**, 93 (1989).

IX.E-10. D.B. Bukur, S.A. Patel and X. Lang, *Appl. Catal.*, **61**, 329 (1990).

11. L. Caldwell and D.S. Van Vuuren, *Chem. Eng. Sci.*, **41**, 89 (1986).

IX.E-12. A.P. Raje and B.H. Davis, Applied Catalysis, (submitted) (1995).

IX.E-13. R. B. Anderson, ""

IX.E-14. R.C. Wilhoit and B.J. Zwolinski, "Handbook of Vapor Pressures and Heats of Vaporization of Hydrocarbons and Related Compounds", Thermodynamics Research Center, Texas A&M University, College Station, Texas, (1971).

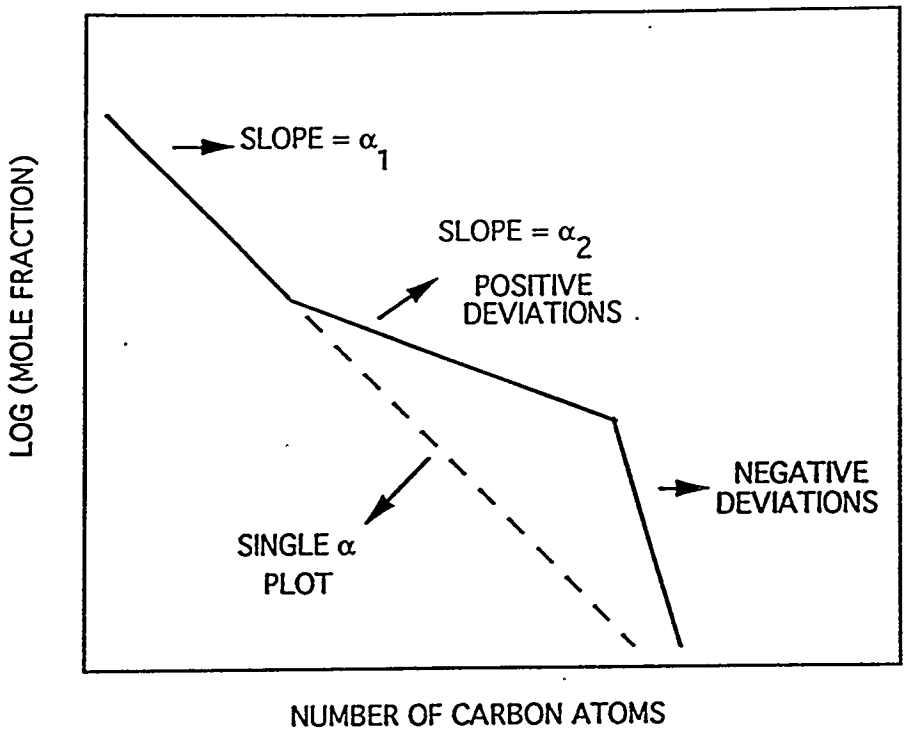

Figure IX.E-1. Schematic diagram of experimentally obtained hydrocarbon selectivity plots.

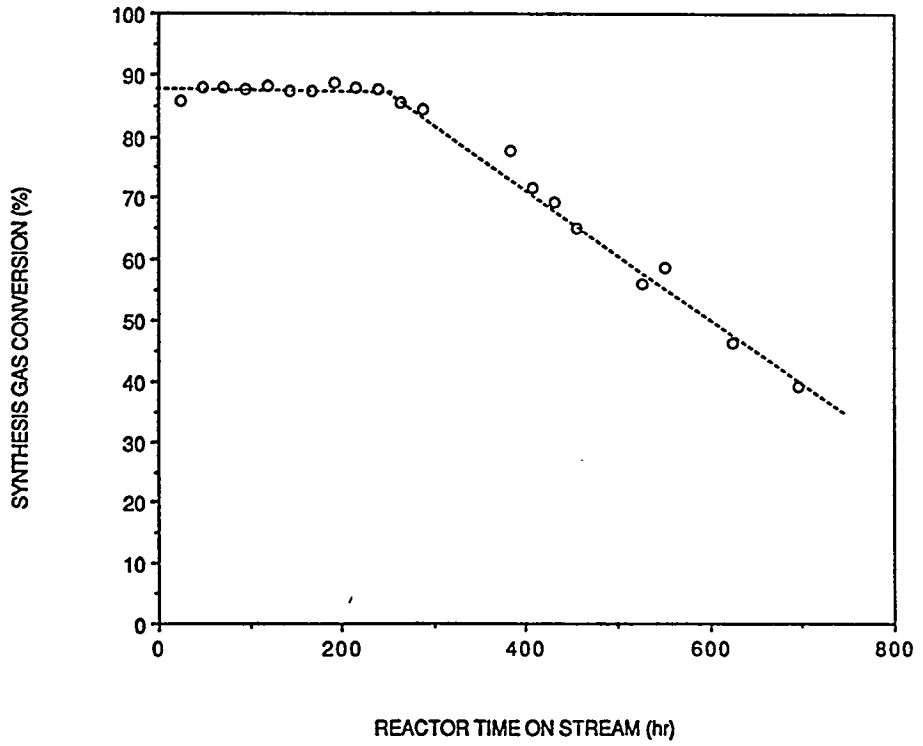

Figure IX.E-2. Experimental synthesis gas conversions as a function of reactor time on stream.

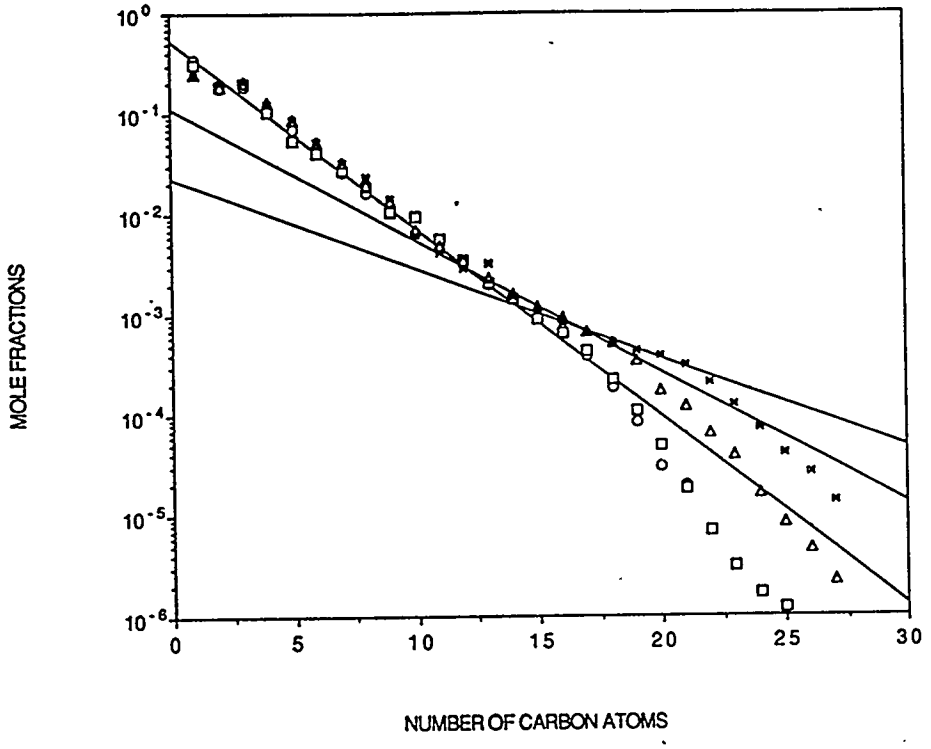

Figure IX.E-3. Experimentally obtained hydrocarbon selectivity plots at various reactor times on stream. (○ at 48 hours; □ at 240 hours; △ at 456 hours; * at 552 hours).

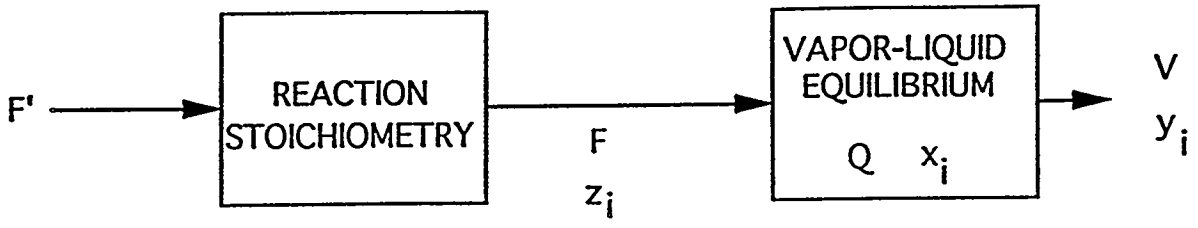

Figure IX.E-4. Schematic diagram of the vapor-liquid equilibrium model. (F': molar flow rate of feed synthesis gas; F: molar flow rate after reaction; z_i: mole fraction of individual hydrocarbons; Q: moles of reactor liquid; x_i: mole fractions of individual hydrocarbons in reactor liquid; V: exit vapor molar flow rate; y_i: mole fractions of individual hydrocarbons in exit vapor stream).

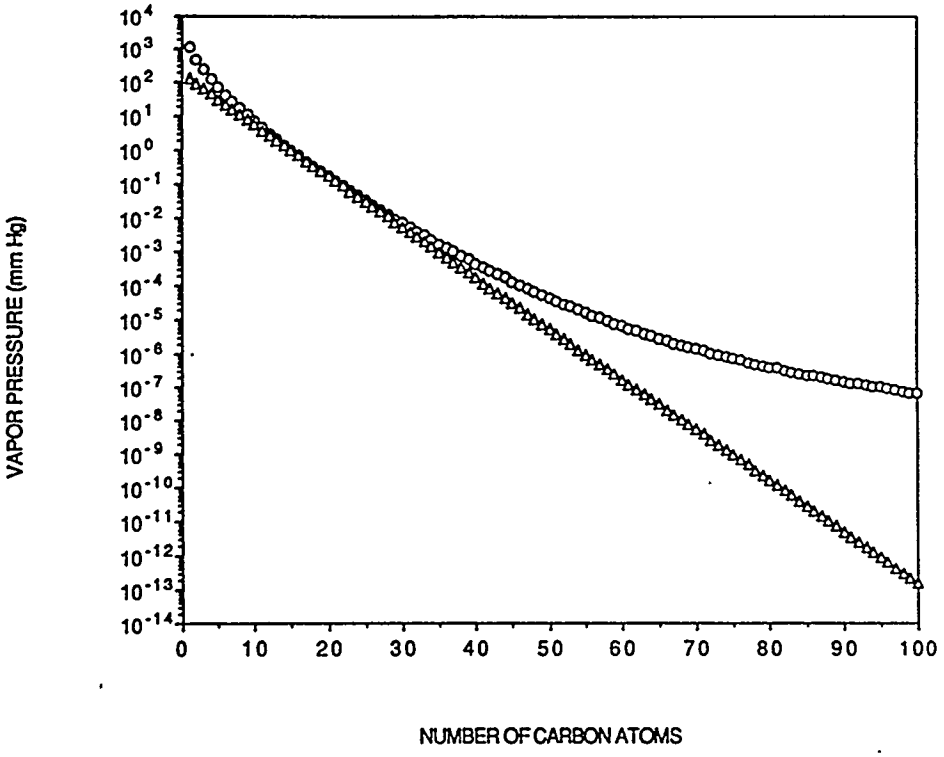

Figure IX.E-5. Comparison of hydrocarbon saturation vapor pressures from two sources. (○ API Project 44 (13); △ from Equation (14)).

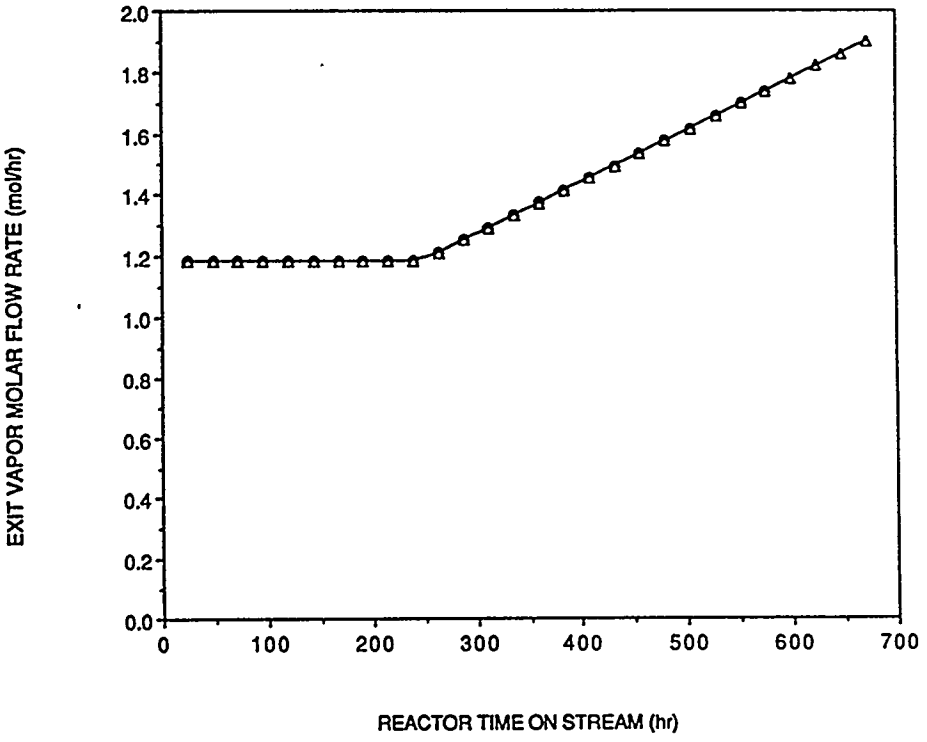

Figure IX.E-6. Exit vapor flow rate from reactor as a function of time on stream. (○ API Project 44 (13); △ from Equation (14)).

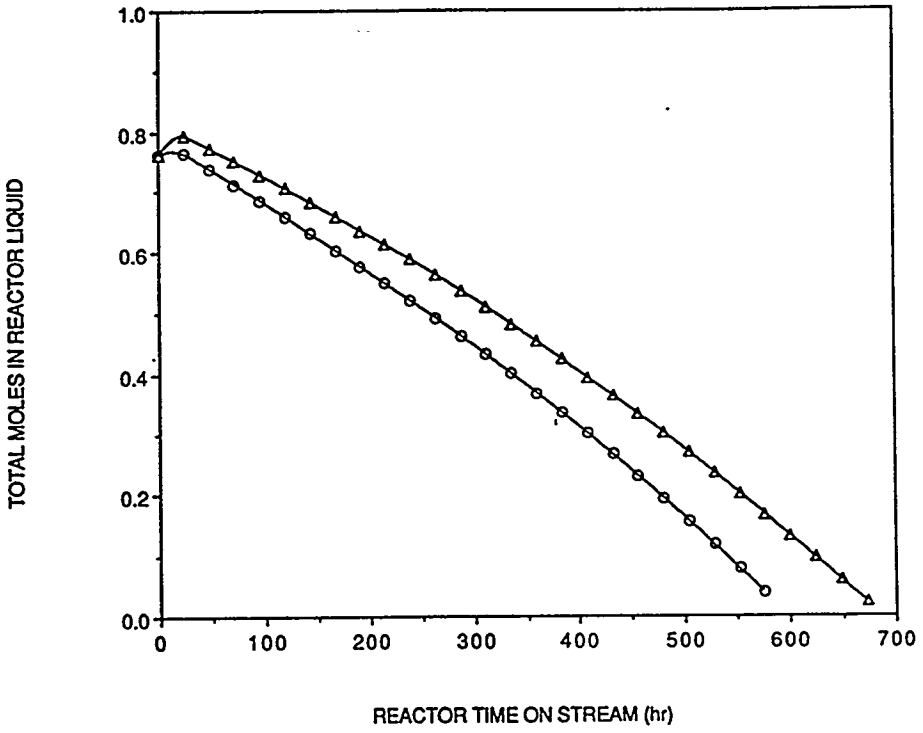

Figure IX.E-7. Moles of liquid remaining in the reactor as a function of time on stream. (○ API Project 44 (13); △ from Equation (14)).

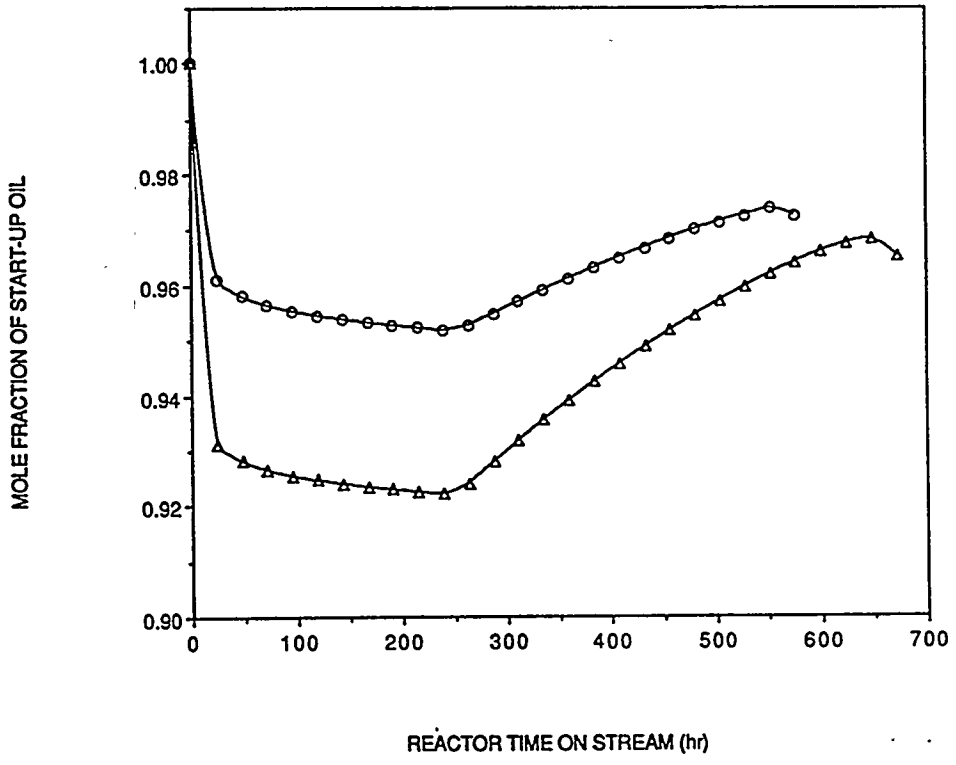

Figure IX.E-8. Mole fraction of start-up oil C_{28} paraffin as a function of time on stream. (○ API Project 44 (13); △ from Equation (14)).

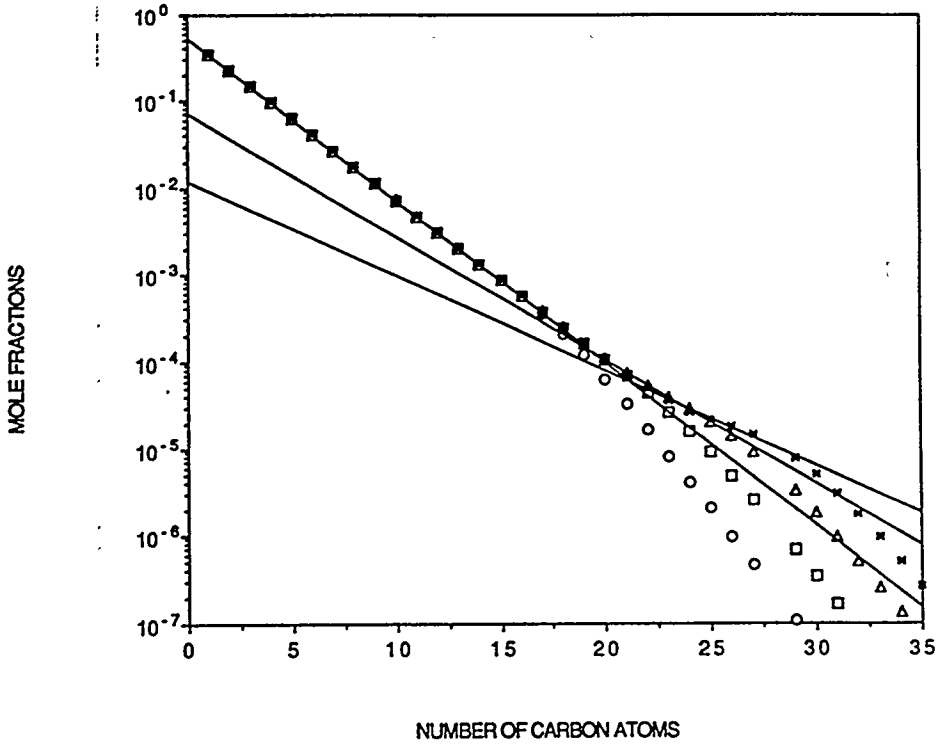

Figure IX.E-9. Vapor phase hydrocarbon mole fractions predicted by VLE model as a function of time on stream using saturation vapor pressures from API Project 44 (13). (○ at 48 hours; □ at 240 hours; △ at 456 hours; * at 552 hours).

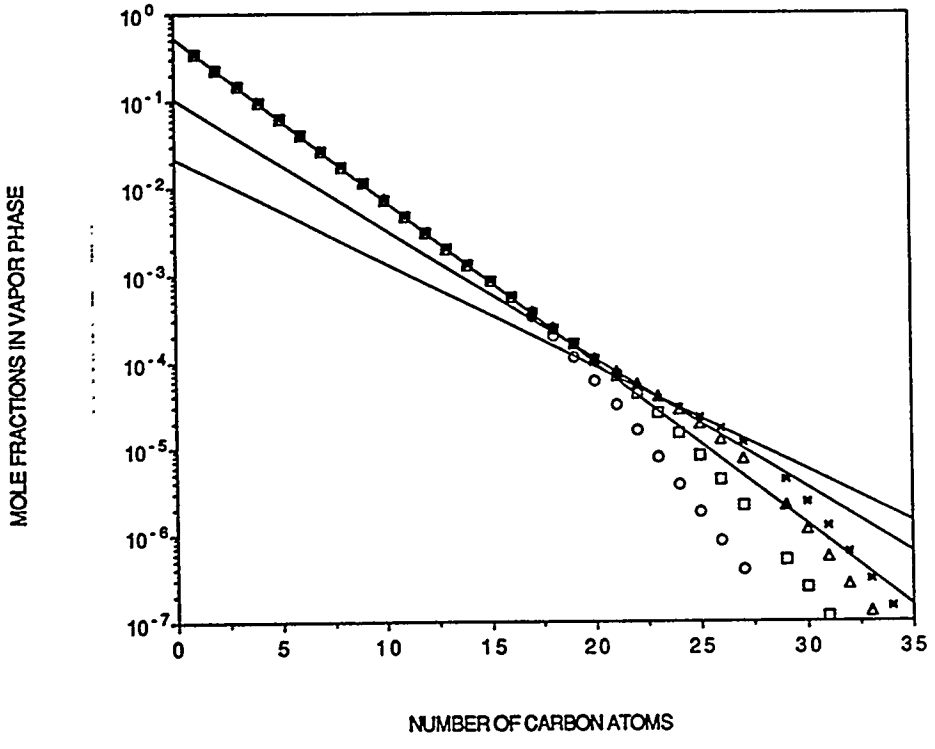

Figure IX.E-10. Vapor phase hydrocarbon mole fractions predicted by VLE model as a function of time on stream using saturation vapor pressures from Equation (14). (○ at 48 hours; □ at 240 hours; △ at 456 hours; * at 552 hours).

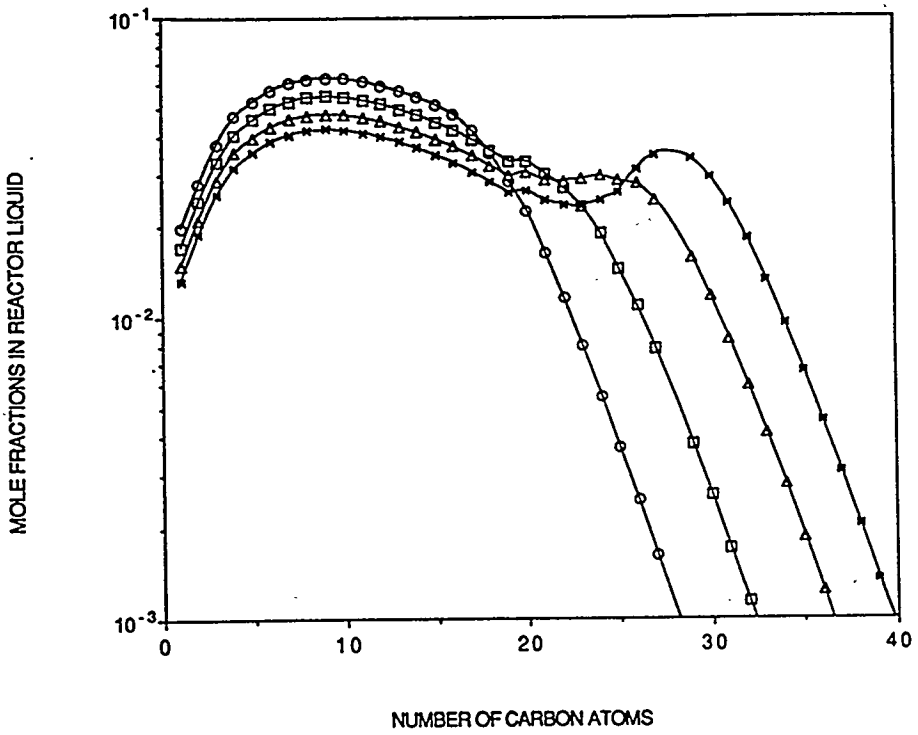

Figure IX.E-11. Mole fractions of hydrocarbons in liquid phase in reactor predicted by VLE model as a function of time on stream using saturation vapor pressures from API Project 44 (13). (○ at 48 hours; □ at 240 hours; △ at 456 hours; * at 552 hours).

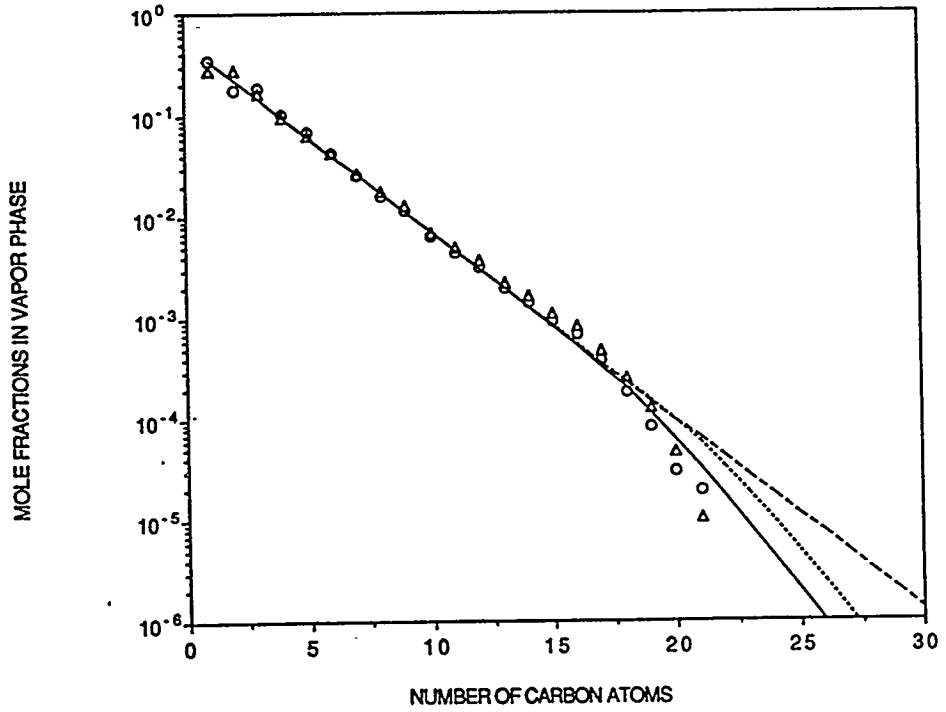

Figure IX.E-12. Comparison of vapor phase hydrocarbon compositions observed experimentally and predicted by the VLE model at a time on stream of 48 and 120 hours. (○ experimental at 48 hours; △ experimental at 120 hours; — predicted at 48 hours; •••• predicted at 120 hours; ---- theoretical ASF plot with a single a = 0.65).

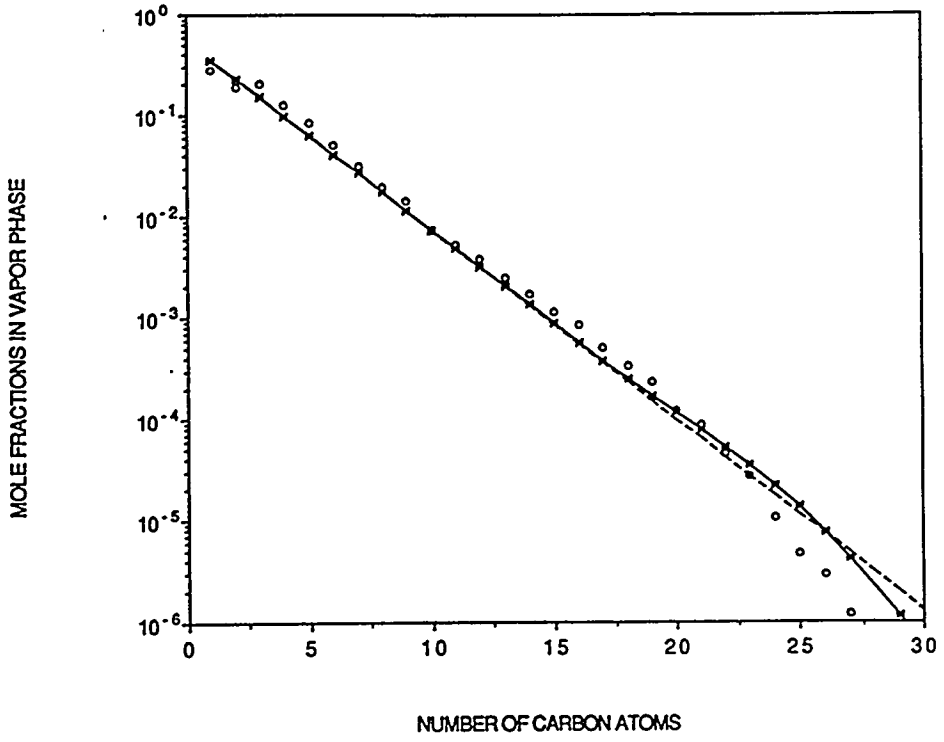

Figure IX.E-13. Comparison of vapor phase hydrocarbon compositions observed experimentally (○) and predicted by the VLE model (*) at a time on stream of 312 hours. --- is the theoretical ASF plot with a single a = 0.65.

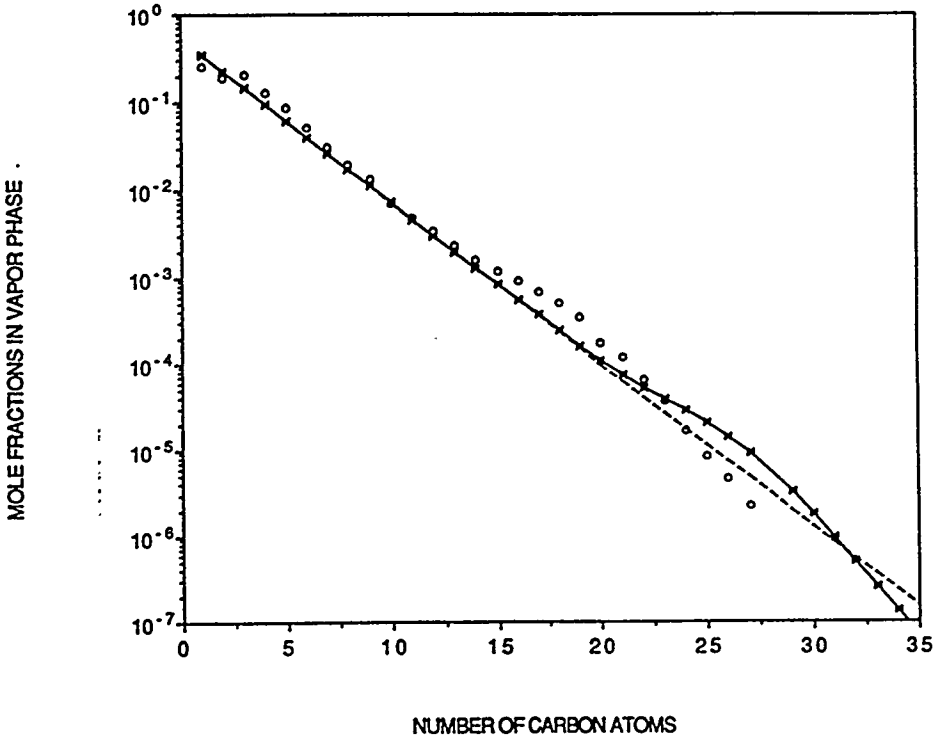

Figure IX.E-14. Comparison of vapor phase hydrocarbon compositions observed experimentally (○) and predicted by the VLE model (*) at a time on stream of 456 hours. --- is the theoretical ASF plot with a single a = 0.65.

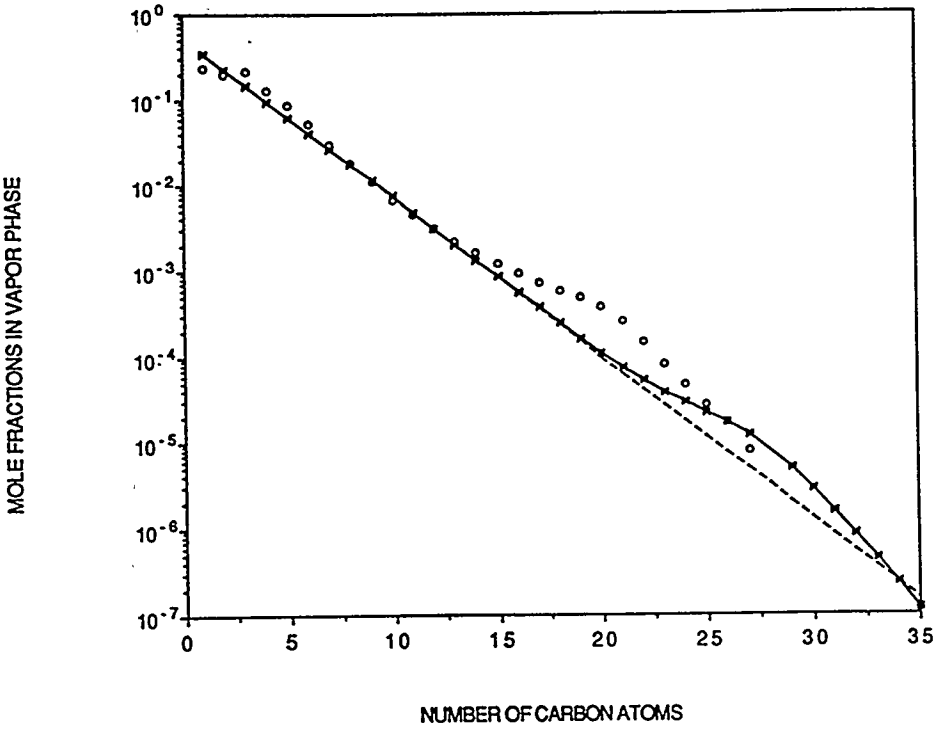

Figure IX.E-15. Comparison of vapor phase hydrocarbon compositions observed experimentally (○) and predicted by the VLE model (*) at a time on stream of 504 hours. --- is the theoretical ASF plot with a single a = 0.65.

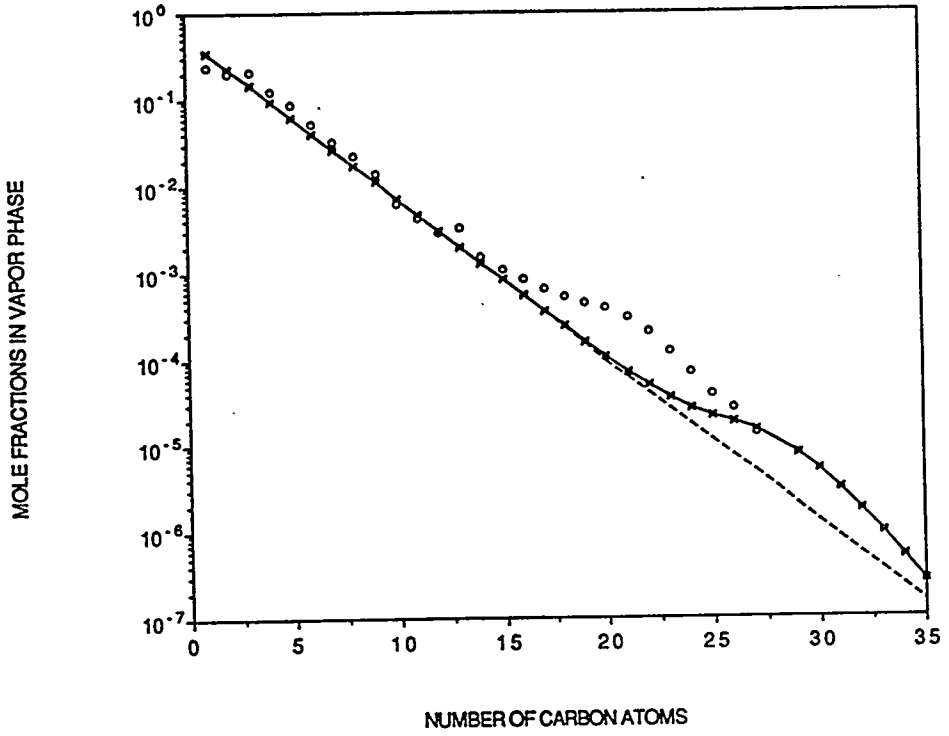

Figure IX.E-16. Comparison of vapor phase hydrocarbon compositions observed experimentally (○) and predicted by the VLE model (*) at a time on stream of 552 hours. --- is the theoretical ASF plot with a single a = 0.65.

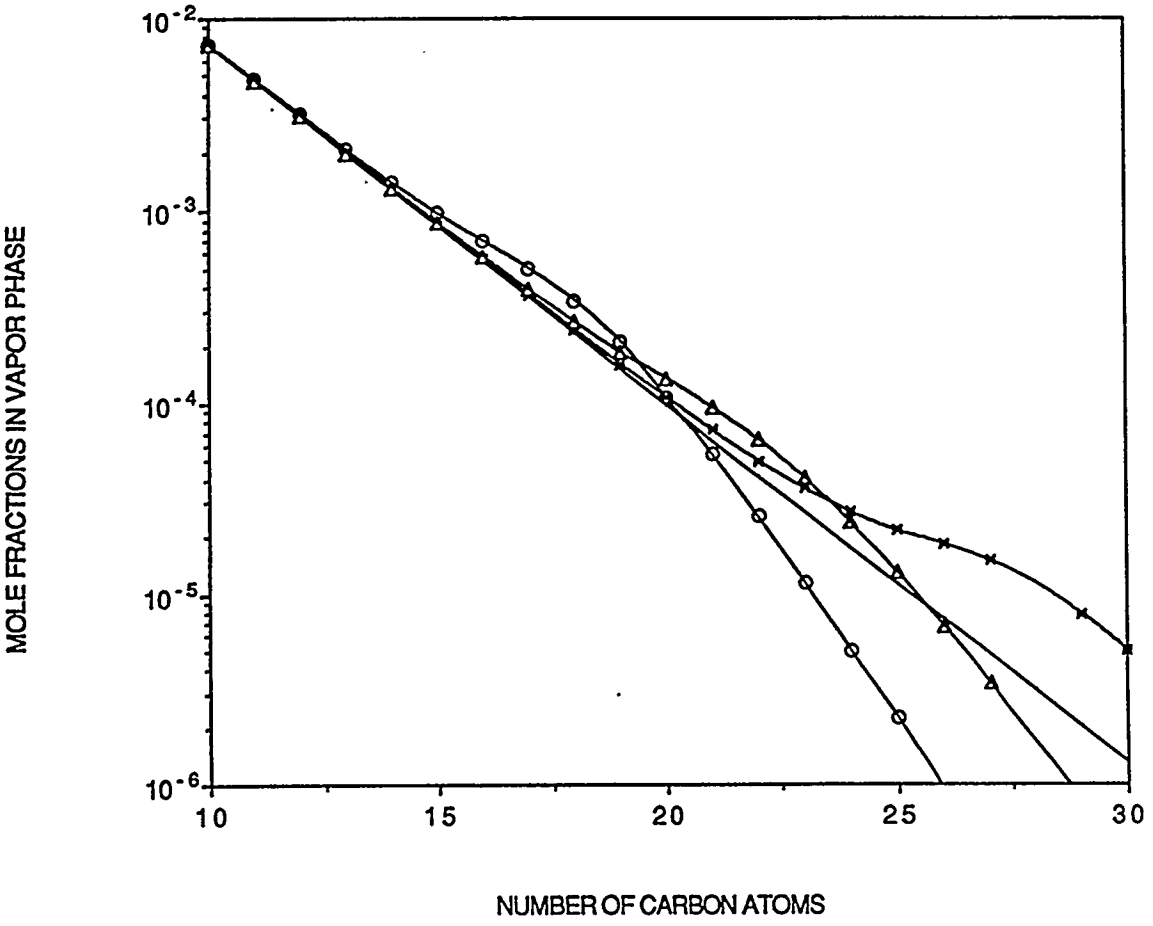

Figure IX.E-17. Comparison of predicted vapor phase hydrocarbon compositions as a function of vapor-liquid equilibrium temperature at a time on stream of 552 hours. (* at 270°C; △ at 240°C; ○ at 200°C; --- is the theoretical ASF plot with a single a = 0.65).